Laser heterodyne radiometers (LHR) for in situ ground-based remote sensing of greenhouse gases in the atmospheric column

Jingjing Wang[1,2], Fengjiao Shen[1], Tu Tan[2], Zhensong Cao[2], Xiaoming Gao[2], Pascal Jeseck[3], Yao Te[3], and Weidong Chen[1]
[1] Laboratoire de Physicochimie de l'Atmosphère, Université du Littoral Côte d'Opale- 59140 Dunkerque, France
[2] Anhui Institute of Optics and Fine Mechanics, Chinese Academy of Sciences, 230031, Hefei, China
[3] Laboratoire d'Etudes du Rayonnement et de la Matière en Astrophysique et Atmosphères Université Pierre et Marie Curie, 75252 Paris, France
* Email : chen@univ-littoral.fr

Introduction

Measurements of vertical concentration profiles of greenhouse gases (GHGs) is extremely important for our understanding of regional air quality and global climate change trends. In this context, laser heterodyne radiometer (LHR) technique has been developed[1-5] for ground-based remote measurements of GHGs in the atmospheric column. Solar radiation undergoing absorption by multi-species in the atmosphere is mixed with a local oscillator (LO) in a photodetector. Beating note at radio frequency (RF) resulted from this photo mixing contains absorption information of the LO-targeted molecules. Scanning the LO frequency across the target molecular absorption lines allows one to extract the corresponding absorption features from the total absorption of the solar radiation by all molecules in the atmosphere. Near-IR (~1.5 µm) and mid-IR (~8 µm)[6] LHRs have been recently developed in the present work. Field campaigns have been performed on the roof of the platform of IRENE in Dunkerque (51.05°N/2.34°E) to measure the CH_4, N_2O, CO_2 (including $^{13}CO_2$ / $^{12}CO_2$), H_2O vapor (and its isotopologue HDO) in the atmospheric column.

Principle of LHR

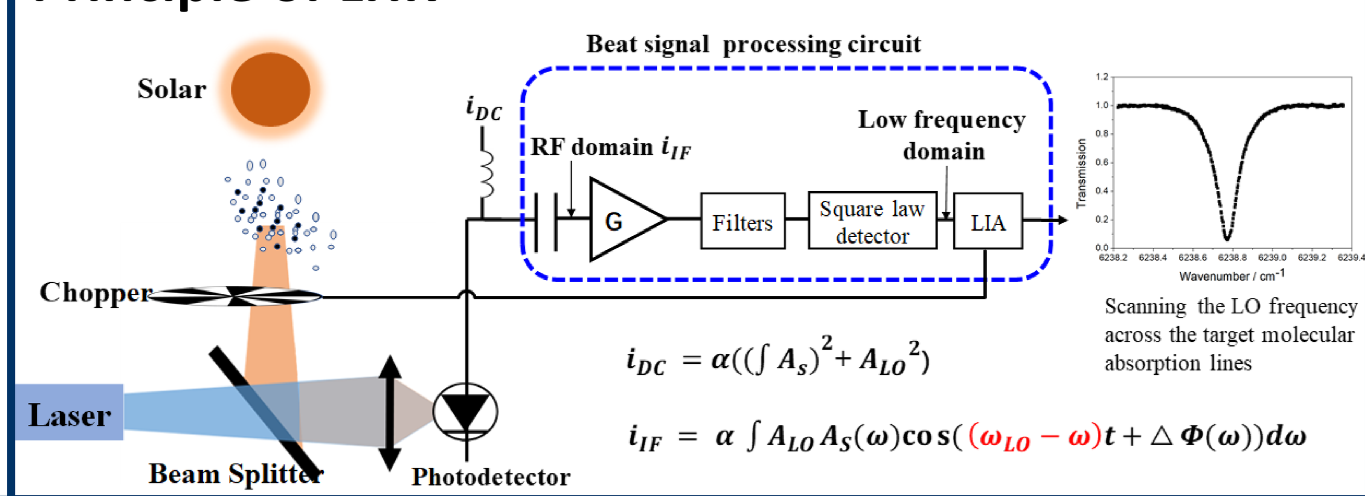

Dual-channel LHR for the simultaneous measurement of CH_4 & CO2

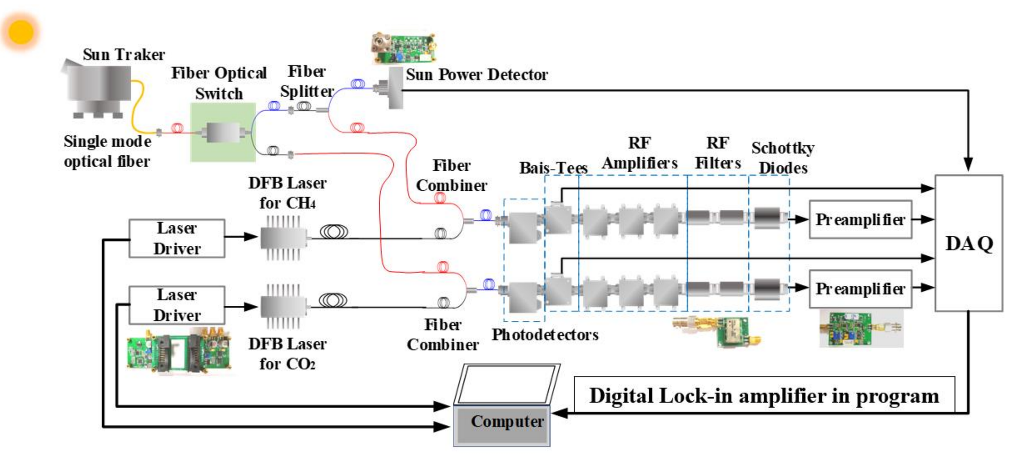

Fig 1: Schematic diagram of the instrument integration principle of the dual-channel LHR.

Fig 2: Physical picture of integrated instrument.

The solar radiation is collected by the sun tracker, then modulated by a 1x2 fiber optical switch. The outputs of two low-cost DFB lasers (1650.9 nm & 1603.6 nm) are combined with the sunlight from the fiber optical switch by fiber combiners and mixed in the photodetectors to generator two beat signals respectively. These signal are processed by beat signal processing circuits and collected by a DAQ to produce the absorption spectrum of sunlight. 5% power of one output of the optical switches is separated by a fiber splitter and it is used to monitor the sunlight intensity by a sun power detector. Among them, the module of lasers driver and temperature control, the sunlight power detector and pre-amplifier are self-made, digital lock-in amplifier is designed in the acquisition program (LabVIEW software is employed)

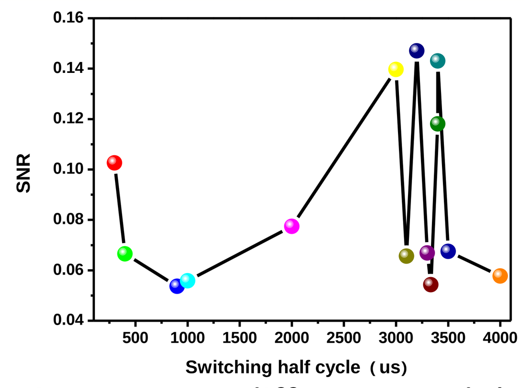

Fig 3: SNR at different modulation frequencies of optical switches.

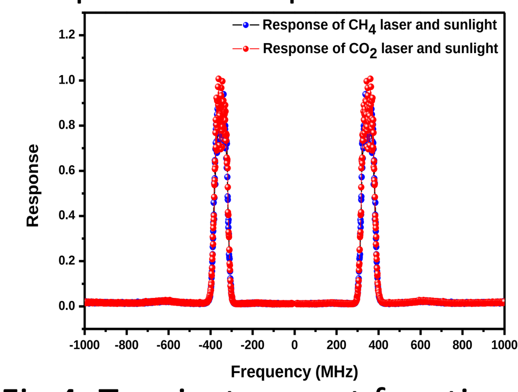

Fig 4: Two instrument functions of LHR.

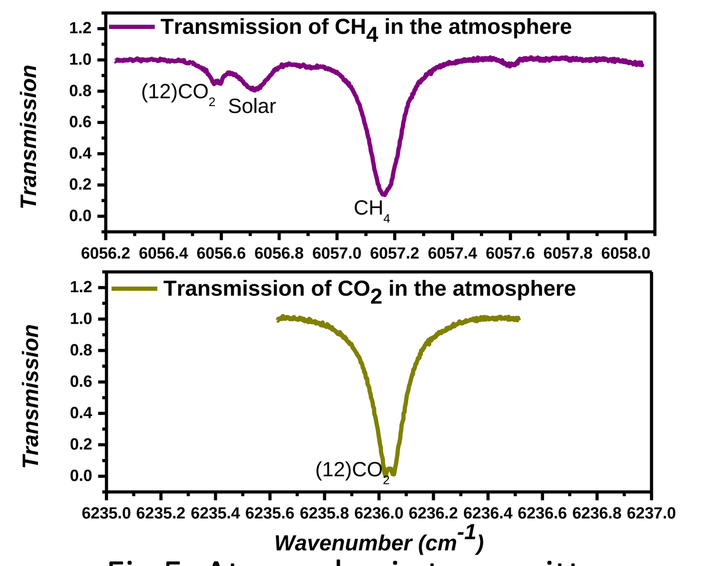

Fig 5: Atmospheric transmittance spectrum of methane and CO2 in the atmosphere.

CH_4 @6057.080 cm^{-1} SNR = 197
CO_2 @6056.508 cm^{-1} SNR = 209
Spectral resolution : ~0.003 cm^{-1}
(in Hefei, China, 31.9° N 117.16° E)

Near-IR LHR for the measurement of CO2 (including $^{13}CO_2$ / $^{12}CO_2$), H2O vapor (and its isotopologue HDO)

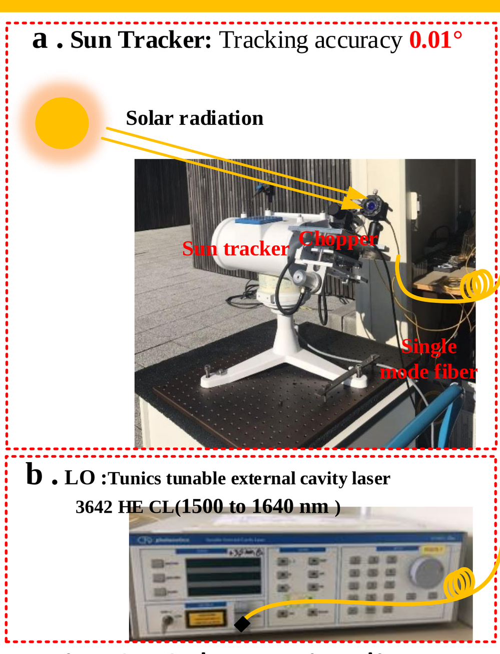

Fig 6: Schematic diagram of measuring device.

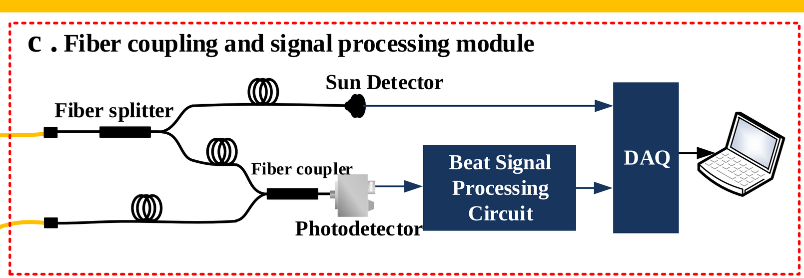

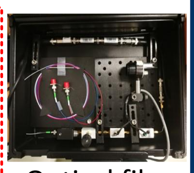

Optical fiber structure

This LHR has similar fiber coupling structure (Fig 6.c) and beat signal processing circuits with the previous setup, but a wide band tunable external cavity laser is used as the LO(Fig 6.b). It has low RF noise(Fig 7). The radiation from the solar tracker (Fig 6.a) and LO is connected to the measurement system by single-mode fiber.

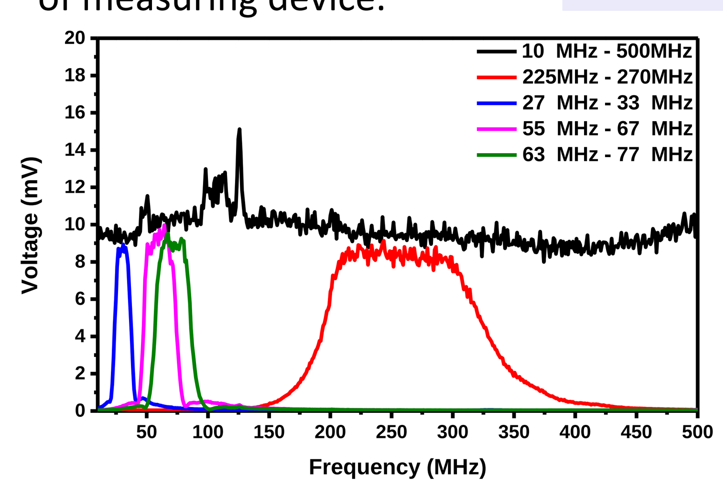

Fig 7: Measurement system RF noise.

Spectral resolution : 0.009 cm^{-1}

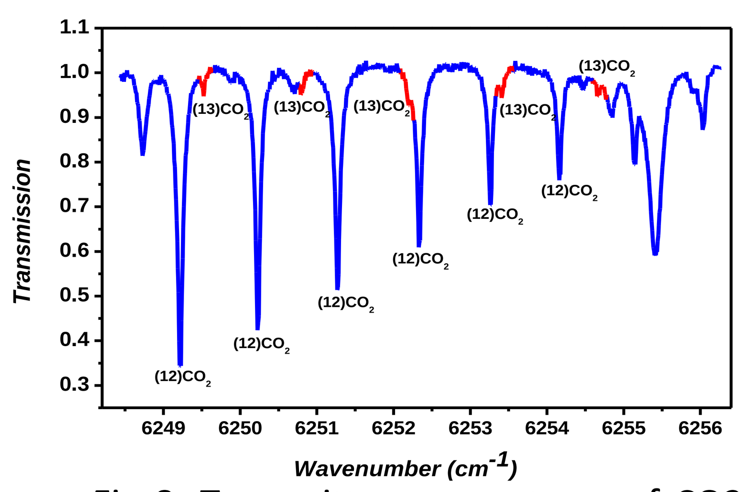

Fig 8: Transmittance spectrum of CO2 in the atmosphere.

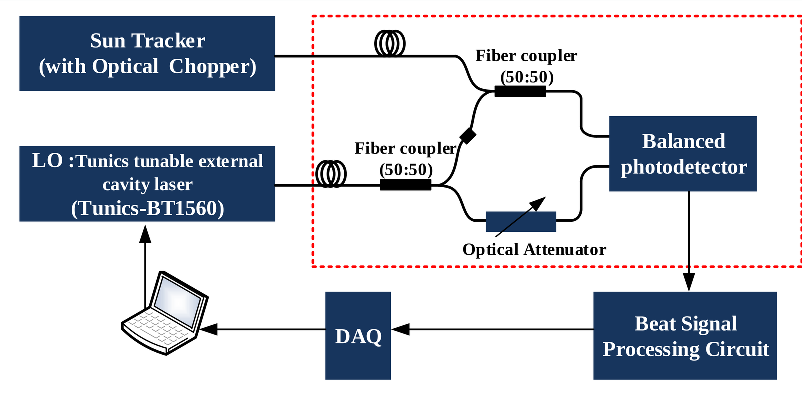

Fig 9:Schematic diagram of laser heterodyne balance detection.

Optical fiber structure

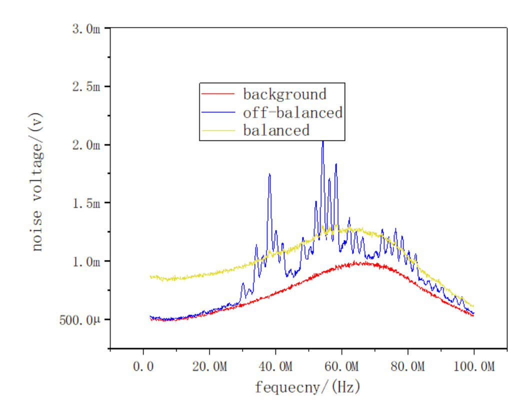

Fig 10: Spectrum in balanced and unbalanced mode.

In this structure (Fig 9), a balanced photo-detector is used, one of it input ports accept the combination of sunlight and LO, another input ports only accept LO. A variable fiber attenuator is used to adjust the optical power in the reference channel of balanced photo-detector. The Spectrums from spectrum analyzer(Fig 10) show balanced detection can reduce RF noise.

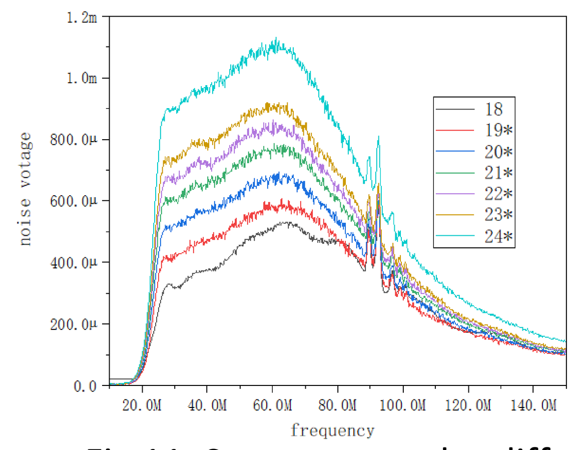

Fig 11: Spectrum under different local oscillator powers.

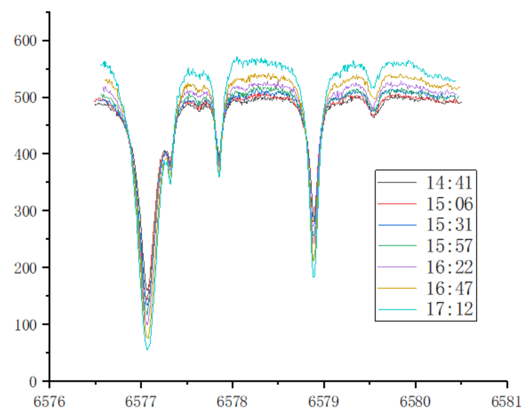

Fig 12: Laser heterodyne signal at different times of one day.

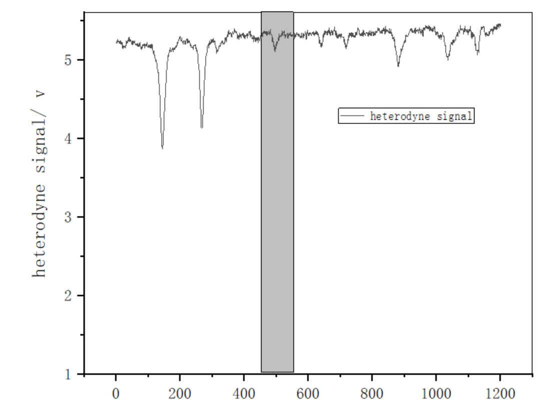

Fig 13: H2O isotope absorption signal measured by LHR.

Mid-IR LHR for the measurement of N_2O

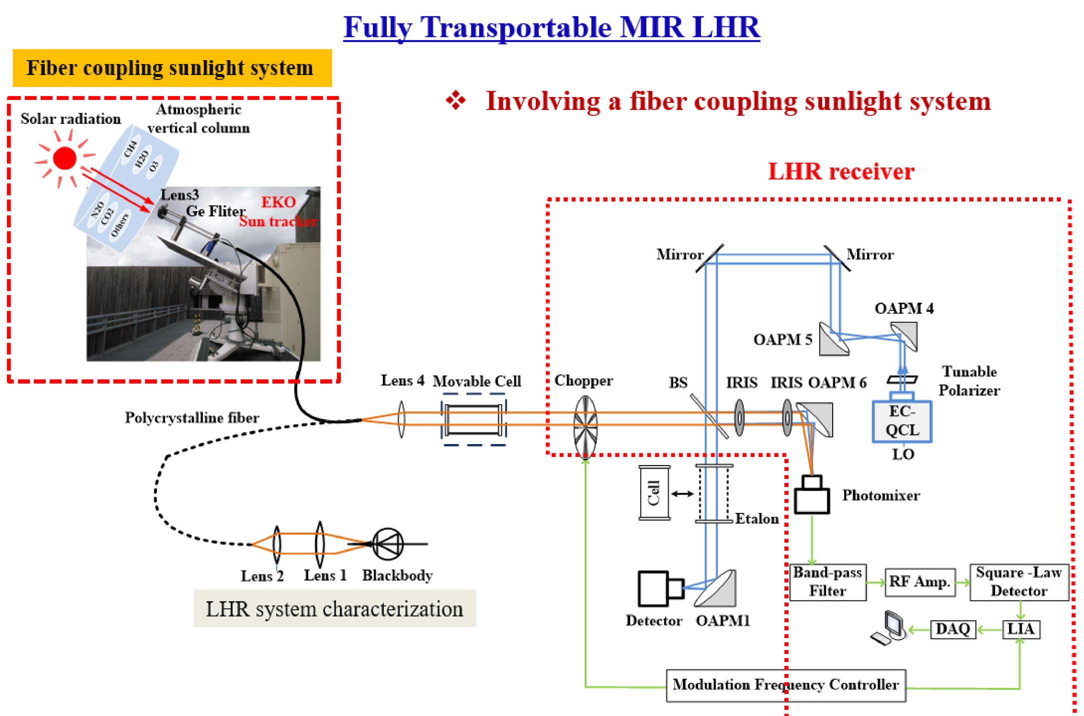

Fig 14: Schematic of the MIR-LHR prototype involving a fiber to couple sunlight to the LHR receiver.

Fig 15: Mid-IR LHR prototype in use for a field measurement test.

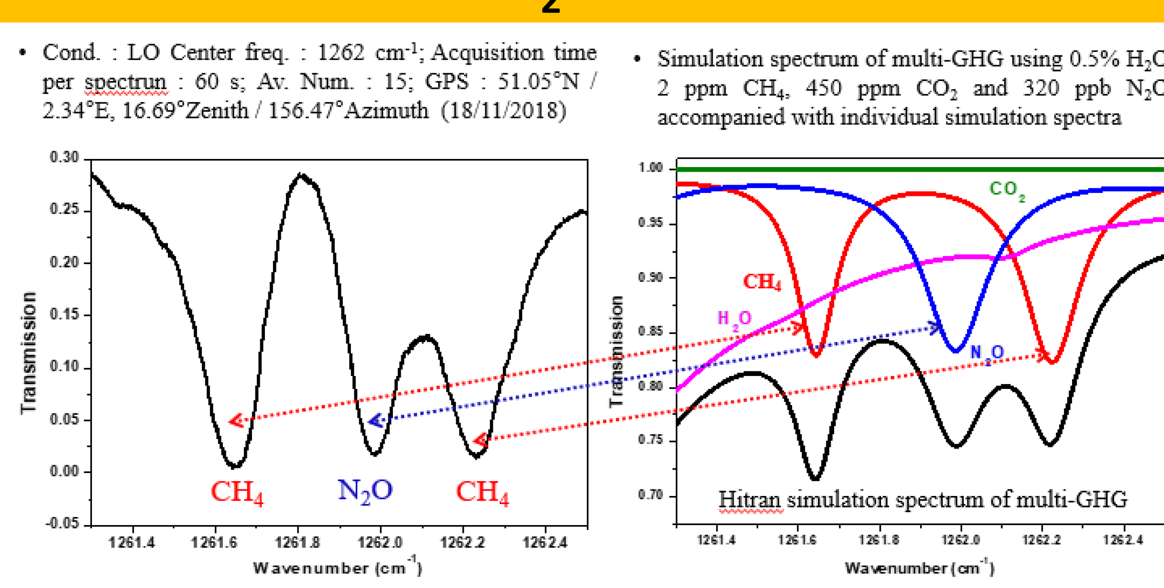

Fig 16: LHR spectrum identification.

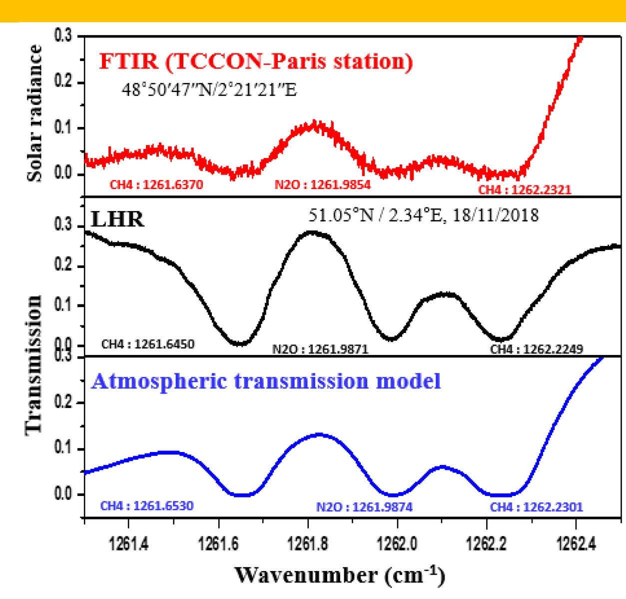

Fig 17: Inter-comparison.

As H_2O is interfering with the LHR spectrum of CH_4-N_2O, and the H_2O distribution changes with time and space → Slightly different in line-shape

Slightly different in line-shape due to H_2O (diff. locations; diff. time; diff. atmospheric conditions) → Consistent in overall spectral line-shape

Conclusions & Perspectives

A dual-channel LHR for the simultaneous measurement of CH_4 & CO_2, a broadband LHR for CO_2($^{13}CO_2$ / $^{12}CO_2$) and a laser heterodyne balance detection device in near IR, and a prototype of mid-IR LHR were developed and tested with ground-based remote measurement of CH_4, N_2O, CO_2 (including $^{13}CO_2$ / $^{12}CO_2$), H_2O vapor (and its isotopologue HDO) in the atmospheric column, on Dunkerque and Hefei. The LHR spectrums were in good agreement with the FT-IR spectrum (Bruker IFS 125HR FTS) and SNR.

- Improve the SNR and ILS of LHR and optimize the laser wavelength correction.
- Development of a heterodyne spectrum inversion algorithm to determine the vertical concentration profile of the target atmospheric trace gases and analyze the reliability of the inversion results.

[1] R. T. Menzies, and R. K. Seals, Science 197 (1977) 1275-1277.
[2] D. Weidmann, T. Tsai, N. A. Macleod, and G. Wysocki, Opt. Lett. 36 (2011) 1951-1953.
[3] E. L. Wilson, M. L. McLinden, and J. H. Miller, Appl. Phys. B 114 (2014) 385-393.
[4] A. Rodin, A. Klimchuk, A. Nadezhdinskiy, D. Churbanov, and M. Spiridonov, Opt. Express 22(2014) 13825-13834.
[5] J. Wang, G. Wang, T. Tan, G. Zhu, C. Sun, Z. CAO, W. Chen, and X. Gao, Opt. Express 27 (2019) 9600-9619.
[6] F. Shen, P. Jeseck, Y. Te, T. Tan, X. Gao, E. Fertein, and W. Chen, Geophys. Res. Abstracts, 20(2018) EGU2018-79.

Acknowledgments

The authors thank the financial supports from the LABEX CaPPA project (ANR-10-LABX005), the MABCaM (ANR-16-CE04-0009) and the MULTIPAS (ANR-16-CE04-0012) contracts, as well as the CPER CLIMIBIO program. S. F. thanks the project Labex CaPPA and the "Pôle Métropolitain de la Côte d'Opale" (PMCO) for the PhD fellowship support.